



1 **A method for the direct measurement of surface tension of**  
2 **atmospherically relevant aerosol particles using atomic**  
3 **force microscopy**

4

5 **A. D. Hritz, T. M. Raymond, and D. D. Dutcher**

6 {Bucknell University, Lewisburg, Pennsylvania}

7 Correspondence to: D. D. Dutcher (dabrina.dutcher@bucknell.edu)

8



## 1 **Abstract**

2 Accurate estimates of particle surface tension are required for models concerning atmospheric  
3 aerosol nucleation and activation. However, it is difficult to collect sufficiently large volumes  
4 of atmospheric aerosol for use in typical instruments that measure surface tension, such as  
5 goniometers or Wilhelmy plates. In this work, a method that measures the surface tension of  
6 collected liquid nanoparticles using atomic force microscopy is presented. A film of particles  
7 is collected via impaction and is probed using nanoneedle tips with the atomic force  
8 microscope. This micro-Wilhelmy method allows for direct measurements of surface tension  
9 of small amounts of sample.

10 This method was verified using liquids whose surface tensions were known. Particles of  
11 oxidized  $\alpha$ -pinene were then produced, collected, and analyzed using this method. Preliminary  
12 results show that oxidized  $\alpha$ -pinene particles formed in dry conditions have a surface tension  
13 similar to that of pure  $\alpha$ -pinene, and particles formed in wet conditions have a surface tension  
14 that is significantly higher.

15

## 16 **1 Introduction**

17 According to the Fifth Assessment Report of the Intergovernmental Panel on Climate Change,  
18 clouds and aerosols contribute the largest uncertainty to understanding changes in climate  
19 (Boucher et al., 2013). Aerosols affect the climate directly by reflecting or absorbing solar  
20 radiation, and indirectly when they form cloud particles (Boucher et al., 2013). A major  
21 difficulty in modeling particle nucleation and aerosol activation lies in determining physical  
22 properties of particles on the nanoscale without precise knowledge about chemical  
23 composition.

24 Recent studies in particle nucleation and cloud droplet activation have used various methods  
25 to estimate particle surface tension, which is a very important parameter in modeling both  
26 processes (Laaksonen and McGraw, 1996; Moldanova and Ljungström, 2000; Wex et al.,  
27 2009; Petters et al., 2009; Duplissy et al., 2008; Kiss et al., 2005). Particle nucleation is  
28 described by the Kelvin equation (Laaksonen and McGraw, 1996), which requires knowledge  
29 about surface tension of the nucleating particle (Laaksonen and McGraw, 1996; Schmelzer et  
30 al., 1996). Not surprisingly, direct measurement of this type of surface tension has not been  
31 possible. Studies on nucleation often rely on an assumption about the composition and use



1 tabulated values for bulk surface tension (Daisey and Hopke, 1993) or simply assume  
2 “physically reasonable values“ (Moldanova and Ljungström, 2000). A direct method of  
3 measuring the surface tensions of particles shortly after nucleation is preferable to these  
4 assumptions and would likely reduce the error in particle nucleation models.

5 Köhler theory is used to predict the properties of activating cloud condensation nuclei  
6 (Köhler, 1936). The Köhler equation balances the Kelvin effect with Raoult’s Law in order to  
7 describe particle activation. Thus, similar problems arise in specifying physical properties  
8 used in the Kelvin term of the Köhler equation. To date, there has been little consistency  
9 between assumptions used for the activated particles’ surface tensions. Many researchers  
10 (Prenni et al., 2007; Petters and Kreidenweis, 2007; Huff Hartz et al., 2005; Conant et al.,  
11 2002) have assumed that, at activation, the particles consist mainly of water, so a surface  
12 tension for pure water was used. Though this is a good initial assumption, it neglects the  
13 depressive effect of organic surfactants on the activating particles’ surface tensions (Kiss et  
14 al., 2005; Facchini et al., 1999). It is now generally agreed upon that, for most activating  
15 particles with these surfactants, the surface tension is reduced by about 10-15% (Facchini et  
16 al., 2000; Engelhart et al., 2008; Awa-Awuku et al., 2010; King et al., 2009). Several methods  
17 have been used to predict this surface tension reduction. Some researchers have collected  
18 particles and diluted them so as to allow for a direct measurement using conventional  
19 instruments (Asa-Awuku et al., 2008; Moore et al., 2008; Schwier et al., 2013; Henning et al.,  
20 2005). These values were then extrapolated back to the initial concentration by fitting them to  
21 a Szyskowski-Langmuir isotherm. Occasionally, surface tensions for the particles have been  
22 back-calculated using Köhler Theory Analysis when all other parameters are known or  
23 estimated (Asa-Awuku et al., 2010; Engelhart et al., 2008). Others (Raymond and Pandis,  
24 2002; Kiss et al., 2005) have prepared solutions mimicking the bulk chemical composition of  
25 aerosol particles and directly measured their surface tensions. However, none of these  
26 methods directly measures the surface tension of the actual particles in question.

27 Yazdanpanah (Yazdanpanah et al., 2008) has developed a method to measure the surface  
28 tension of small (~200 nm in diameter) droplets and films using constant-diameter nanoneedle  
29 tips on the atomic force microscope. In this work, we will show how his method has been  
30 adapted to accurately measure the surface tensions of collected atmospheric aerosols.

31



## 1 **2 Experimental Methods**

2

### 3 **2.1 Particle Generation**

4 In this project, oxidized  $\alpha$ -pinene particles were generated in a 1 m<sup>3</sup> polytetrafluoroethylene  
5 (PTFE) smog chamber (Fig. 1). Particles were formed in either “dry“ (<5% RH) or “wet“  
6 (67% RH) conditions. To generate the “dry“ conditions, the chamber was flushed with clean,  
7 dry air for several hours. To generate the “wet“ conditions, clean air was bubbled through  
8 water at 2 liters per minute (LPM), filtered, and sent to the smog chamber. The chamber was  
9 flushed with this humid air stream until a maximum relative humidity was reached. Relative  
10 humidity was measured using a Vaisala HM337 Humidity and Temperature Transmitter.

11 During experiments, the dry air stream was sent into the smog chamber at 2 LPM. This air  
12 stream could be diverted either through a sample port or through an ozone generator  
13 (Poseidon Ozone Generator by Ozotech) in series with a HEPA filter before entering the  
14 chamber. An outlet port from the chamber could be connected either to a scanning mobility  
15 particle sizer (a 3080 TSI Differential Mobility Analyzer in series with the 3775 TSI  
16 Condensation Particle Counter) or a cascade impactor (I-1L Cascade impactor by PIXE).  
17 Experiments were only conducted when the initial particle concentration in the smog chamber  
18 was below 100 particles/cm<sup>3</sup>, as measured by the scanning mobility particle sizer (SMPS).

19 At the start of each experiment, ozone was added to the smog chamber. If particle counts in  
20 the smog chamber remained low after about five minutes, indicating a chamber free of  
21 oxidizable volatile organic compounds, 5  $\mu$ L of liquid  $\alpha$ -pinene (97% pure, Acros Organics)  
22 was then injected into a sample port, where it was vaporized and carried into the smog  
23 chamber. Ozone and  $\alpha$ -pinene were added in a roughly 1:1 molar ratio; the high starting  
24 concentrations were necessary so that an adequate particle volume would form for collection  
25 later. The resulting oxidized  $\alpha$ -pinene particles were allowed to age in the chamber for 90  
26 minutes.

27 During the aging process, particle size distribution data was collected with the SMPS. The  
28 SMPS sample flowrate was 0.3 LPM and the sheath flowrate used on the Differential  
29 Mobility Analyzer (DMA) was 3 LPM. These settings allowed for collection of particle size  
30 distribution data over the range of 15 to 660 nm. The low sampling flowrate ensured that the  
31 smog chamber operated under positive pressure. The size of the oxidized  $\alpha$ -pinene particles



1 followed a log-normal distribution whose center shifted to larger sizes over time. In the period  
2 where particles aged, the modal diameter increased from around 120 to 200 nm. The most  
3 significant changes in particle size distribution occurred in the first hour after the  $\alpha$ -pinene  
4 was introduced to the smog chamber. Particles were left to age for 90 minutes in order to  
5 minimize changes in particle size distribution during collection.

6

## 7 **2.2 Particle Collection**

8 Ninety minutes after  $\alpha$ -pinene was introduced to the smog chamber, the outlet of the chamber  
9 was switched to feed to the cascade impactor. The second smallest stage (L2) was used to  
10 collect the particles on a cleaned steel disk. The 50% aerodynamic cutoff diameter for this  
11 stage at 4 LPM was 40 nm. After 90 minutes a visible particle film had collected on the disk.  
12 Immediately after collection, the sample disk was analyzed using atomic force microscopy  
13 (AFM).

14

## 15 **2.3 Sample Analysis**

16 A Veeco Multimode V Atomic Force Microscope (AFM) and NugaNeedle NN-HAR-FM60  
17 probes were used to analyze the particle film collected on the disk. The probes consist of a  
18 flat, flexible cantilever, and a nanoneedle mounted normally to the cantilever at its end. The  
19 Ga-Ag nanoneedles are shaped as cylinders on the order of 100 nm in diameter and 10  $\mu$ m in  
20 length. A micro-Wilhelmy method was used to measure surface tensions (Yazdanpanah et al.,  
21 2008).

22 The sample was analyzed with the AFM in force mode. In this mode, the AFM's piezoelectric  
23 transducers push the sample film up to and away from the probe with high precision. The  
24 downward force exerted on the probe was recorded by the AFM as a function of its location  
25 relative to the film's surface. A force curve obtained with the AFM is presented in Fig. 2.

26 In Fig. 2, the curve in blue illustrates the force exerted on the probe as it approaches and  
27 touches the sample surface. The curve in red illustrates the force exerted on the probe as it is  
28 pulled from the sample. If it is assumed that only forces related to the surface tension of the  
29 liquid film are exerted on the probe, then equation 1 holds:



1 
$$F_{probe} = \sigma * L * \cos(\theta)$$
 (1)

2

3 where  $\sigma$  is the surface tension of the sample,  $L$  is the wetted perimeter of the tip, and  $\theta$  is the  
4 contact angle between the fluid and the tip.

5 Because the nanoneedle has a cylindrical geometry, the wetted perimeter,  $L$ , is constant  
6 during all force measurements. This can be seen by the near-constant negative force exerted  
7 on the probe when it is initially retracting out of the sample. The increase in the downward  
8 force before the nanoneedle is completely pulled from the sample is attributed to a decrease in  
9 the contact angle. At the point the sample breaks away from the nanoneedle, the contact angle  
10 is zero. When this angle is zero and the needle is smaller than the capillary length (Uddin et  
11 al., 2011), equation 2 holds:

12

13 
$$\sigma = \frac{F_{probe}}{L}$$
 (2)

14

15 For this project, equation 2 was used, using the force reading at the point the nanoneedle  
16 broke from the sample. This corresponds to point 5 in Figure 2.

17 Several aspects of the AFM system were calibrated daily before the collected  $\alpha$ -pinene  
18 particles were analyzed, typically during particle collection. Because the AFM directly  
19 measures deflection of the cantilever, a force exerted on the nanoneedle could only be  
20 obtained after calibrating the cantilever's deflection and determining its spring constant. In  
21 the AFM, a laser is reflected off of the cantilever into a photodetector; cantilever deflection is  
22 measured by movement of the laser on the photodetector. To calibrate this measurement, the  
23 probe was gently pushed into a hard, steel surface. The slope of the force curve when the  
24 probe is in contact with the surface indicates the observed cantilever deflection from the  
25 photodetector (y-axis of the force curve) versus the actual distance the surface is moving the  
26 cantilever (x-axis of the force curve). This slope was entered into the AFM's operating  
27 program.



1 The spring constant of the tip was found using a thermal tune. The thermal tune is a common  
2 method to calculate spring constant using measurements of the cantilever's response to  
3 thermal noise (Serry, 2010). The native Veeco software was used to perform the thermal tune.  
4 After these calibrations, the AFM will produce force curves that relate force and distance  
5 accurately.

6 In order to calculate surface tension from force data, the wetted perimeter of the nanoneedle  
7 also had to be obtained. This was done by obtaining force curves of liquid standards and using  
8 equation 2 to back-calculate the wetted perimeter given force and surface tension information.  
9 Two liquid standards were used: 90% pure oleic acid (Sigma-Aldrich) and 97% pure, non-  
10 oxidized liquid  $\alpha$ -pinene. The surface tensions of these two standards were measured using a  
11 Wilhelmy plate (Sigma 703D, KSV Instruments Ltd.); results are shown in Table 1.  
12 Measurements for the standards yielded lower values compared to the literature for pure oleic  
13 acid and  $\alpha$ -pinene. Because the standards were not completely pure, this was not unexpected,  
14 and surface tension values obtained from the Wilhelmy plate were used.

15 A summary of the steps used to calibrate and analyze samples on the AFM is shown in Figure  
16 3.

17

### 18 **3 Results and Discussion**

19 Surface tension data was obtained for oxidized  $\alpha$ -pinene particles. The AFM's measurements  
20 and calculated values are presented in Table 2. Both "dry" oxidized  $\alpha$ -pinene particles and  
21 "wet" oxidized  $\alpha$ -pinene particles were analyzed. The mean surface tension of "dry" oxidized  
22  $\alpha$ -pinene particles was found to be  $27.5 \text{ dyn cm}^{-1}$  at 23 degrees C, with an average  
23 uncertainty of  $1.1 \text{ dyn cm}^{-1}$ . This is similar to the surface tension of pure  $\alpha$ -pinene as reported  
24 in the literature (Daisey and Hopke, 1993) and measured with our Wilhelmy plate. The mean  
25 surface tension of "wet" oxidized  $\alpha$ -pinene particles was found to be  $44.4 \text{ dyn cm}^{-1}$  at 23  
26 degrees C, with an uncertainty of  $2.4 \text{ dyn cm}^{-1}$ .

27 Table 3 compares the mean surface tensions of oxidized  $\alpha$ -pinene particles measured in this  
28 study with published estimates for the surface tension of activating  $\alpha$ -pinene particles  
29 (Engelhart et al., 2008; Huff Hartz et al., 2005; Prenni et al., 2007). Our results suggest that  
30 the surface tension of dry oxidized  $\alpha$ -pinene particles is not very different from the surface  
31 tension of its VOC precursor. It is also apparent that the surface tension of oxidized  $\alpha$ -pinene



1 particles formed in more humid conditions had a higher surface tension than oxidized  $\alpha$ -  
2 pinene particles formed in dry conditions.

3 These results appear to be in agreement with current theory. It is generally believed that the  
4 surface tension of an activating oxidized  $\alpha$ -pinene particle is slightly lower than that of pure  
5 water, at  $61.7 \text{ dyn cm}^{-1}$  (Engelhart et al., 2008). This is due to the depressive effect of organic  
6 surfactants in the droplets. Our results suggest that the surface tension of particles with a  
7 greater surfactant to water ratio is even lower, somewhere between the surface tension of pure  
8 water and the surface tension of the dry oxidized  $\alpha$ -pinene. Furthermore, the surface tension  
9 of the dry oxidized  $\alpha$ -pinene particles was found to be similar to the surface tension of pure  $\alpha$ -  
10 pinene. This may be due to their similar structures. Now that a method suitable for the direct  
11 measurement of particle surface tension has been established, direct measurements of  
12 particles with several other moisture contents should be taken to examine the precise  
13 relationship between surface tension and moisture content in a particle. With minor  
14 modifications to the particle generation technique, this method can be used to experimentally  
15 measure the surface tension of activating particles.

16

#### 17 **4 Conclusions**

18 A method was developed to measure the surface tension of collected liquid aerosol particles  
19 using atomic force microscopy. Particles are impacted on a clean surface until a film is  
20 formed, then probed with a clean tip in an atomic force microscope. This method minimizes  
21 processing of the particles and therefore reduces the risk of sample contamination. The  
22 method was verified and calibrated using standard liquids whose surface tensions were in the  
23 range of the sample specimens. The standard liquid surface tensions were checked with a  
24 Wilhelmy plate.

25 Relatively dry, oxidized  $\alpha$ -pinene particles were found to have a surface tension similar to that  
26 of pure liquid  $\alpha$ -pinene. Oxidized  $\alpha$ -pinene particles with higher moisture content were found  
27 to have a surface tension significantly higher than that of pure  $\alpha$ -pinene, but lower than  
28 current assumptions for the surface tension of activating oxidized  $\alpha$ -pinene particles. These  
29 preliminary results are consistent with the assumption of surface tension depression currently  
30 used to approximate the surface tension of activating aerosol particles. With simple  
31 modifications to the particle generation technique, this method can be used to experimentally  
32 measure the surface tension of particles at activation.





1

2 **Acknowledgements**

3 The authors thank NaugaNeedles and Dr. Mehdi Yazdanpanah for supplying the tips for the  
4 atomic force microscope and assisting in developing the methods described in this paper. The  
5 authors also thank Drs. James Maneval and Ray Dagastine for their assistance.

6



## 1 **References**

- 2 Asa-Awuku, A., Sullivan, A. P., Hennigan, C. J., Weber, R. J. and Nenes, A.: Investigation of  
3 molar volume and surfactant characteristics of water-soluble organic compounds in biomass  
4 burning aerosol, *Atmos. Chem. Phys.*, 8, 799-812, 2008.
- 5 Asa-Awuku, A., Nenes, A., Gao, S., Flagan, R. C. and Seinfeld, J. H.: Water-soluble SOA  
6 from Alkene ozonolysis: composition and droplet activation kinetics inferences from analysis  
7 of CCN activity, *Atmos. Chem. Phys.*, 10, 1585-1597, 2010.
- 8 Boucher, O., Randall, D., Artaxo, P., Bretherton, C., Feingold, G., Forster, P., Kerminen, V.  
9 M., Kondo, Y., Liao, H., Lohmann, U., Rasch, P., Satheesh, S. K., Sherwood, S., Stevens, B.  
10 and Zhang, X. Y.: Clouds and Aerosols, in: *Climate Change 2013: The Physical Science  
11 Basis. Contribution of Working Group I to the Fifth Assessment Report of the  
12 Intergovernmental Panel on Climate Change*, Cambridge University Press, Cambridge, United  
13 Kingdom, 571-657, 2013.
- 14 Conant, W. C., Nenes, A. and Seinfeld, J. H.: Black carbon radiative heating effects on cloud  
15 microphysics and implications for the aerosol indirect effect 1. Extended Kohler theory, *J.  
16 Geophys. Res.*, 107, 4604-4612, 2002.
- 17 Daisey, J. M. and Hopke, P. K.: Potential for Ion-induced Nucleation of Volatile Organic  
18 Compounds by Radon Decay in Indoor Environments, *Aerosol Sci. Tech.*, 19, 80-93, 1993.
- 19 Duplissy, J., Gysel, M., Alfarra, M. R., Dommen, J., Metzger, A., Prevot, A. S. H.,  
20 Weingartner, E., Laaksonen, A., Raatikainen, T., Good, N., Turner, S. F., McFiggans, G. and  
21 Baltensperger, U.: Cloud forming potential of secondary organic aerosol under near  
22 atmospheric conditions, *Geophys. Res. Lett.*, 35, L03818, 2008.
- 23 Engelhart, G. J., Asa-Awuku, A., Nenes, A. and Pandis, S. N.: CCN activity and droplet  
24 growth kinetics of fresh and aged monoterpene secondary organic aerosol, *Atmos. Chem.  
25 Phys.*, 8, 3937-3949, 2008.
- 26 Facchini, M. C., Mircea, M., Fuzzi, S. and Charlson, R. J.: Cloud albedo enhancement by  
27 surface-active organic solutes in growing droplets, *Nature*, 401, 257-259, 1999.



- 1 Facchini, M. C., Decesari, S., Mircea, M., Fuzzi, S. and Loglio, G.: Surface tension of  
2 atmospheric wet aerosol and cloud/fog droplets in relation to their organic carbon content and  
3 chemical composition, *Atmos. Environ.*, 34, 4853-4857, 2000.
- 4 Henning, S., Rosenørn, T., D'Anna, B., Gola, A. A., Svenningsson, B. and Bilde, M.: Cloud  
5 droplet activation and surface tension of mixtures of slightly soluble organics and inorganic  
6 salt, *Atmos. Chem. Phys.*, 5, 575-582, 2005.
- 7 Huff Hartz, K. E., Rosenørn, T., Ferchak, S. R., Raymond, T. M., Bilde, M., Donahue, N. M.  
8 and Pandis, S. N.: Cloud condensation nuclei activation of monoterpene and sesquiterpene  
9 secondary organic aerosol, *J. Geophys. Res.*, 110, D14208, 2005.
- 10 King, S. M., Rosenørn, T., Shilling, J. E., Chen, Q. and Martin, S. T.: Increased cloud  
11 activation potential of secondary organic aerosol for atmospheric mass loadings, *Atmos.*  
12 *Chem. Phys.*, 9, 2959-2972, 2009.
- 13 Kiss, G., Tombácz, E. and Hansson, H.: Surface Tension Effects of Humic-Like Substances in  
14 the Aqueous Extract of Tropospheric Fine Aerosol, *J. Atmos. Chem.*, 50, 279-294, 2005.
- 15 Köhler, H.: The nucleus in and the growth of hygroscopic droplets, *Transactions of the*  
16 *Faraday Society*, 32(2), 1152-1161, 1936.
- 17 Laaksonen, A. and McGraw, R.: Thermodynamics, gas-liquid nucleation, and size-dependent  
18 surface tension, *Europhys. Lett.*, 35, 367-372, 1996.
- 19 Moldanova, J. and Ljungström, E.: Modelling of Particle Formation From NO<sub>3</sub> Oxidation of  
20 Selected Monoterpenes, *J. Aerosol Sci.*, 31, 1317-1333, 2000.
- 21 Moore, R. H., Ingall, E. D., Sorooshian, A. and Nenes, A.: Molar mass, surface tension, and  
22 droplet growth kinetics of marine organics from measurements of CCN activity, *Geophys.*  
23 *Res. Lett.*, 35, 2008.
- 24 Petters, M. D. and Kreidenweis, S. M.: A single parameter representation of hygroscopic  
25 growth and cloud condensation nucleus activity, *Atmos. Chem. Phys.*, 7, 1961-1971, 2007.



- 1 Petters, M. D., Wex, H., Carrico, C. M., Hallbauer, E., Massling, A., McMeeking, G. R.,  
2 Poulain, L., Wu, Z., Kreidenweis, S. M. and Stratmann, F.: Towards closing the gap between  
3 hygroscopic growth and activation for secondary organic aerosol- Part 2: Theoretical  
4 approaches, Atmos. Chem. Phys., 9, 3999-4009, 2009.
- 5 Prenni, A. J., Petters, M. D., Kreidenweis, S. M., DeMott, P. J. and Ziemann, P. J.: Cloud  
6 droplet activation of secondary organic aerosol, J. Geophys. Res., 112, D10223, 2007.
- 7 Raymond, T. M. and Pandis, S. N.: Cloud activation of single-component organic aerosol  
8 particles, J. Geophys. Res., 107, 4787-4794, 2002.
- 9 Schmelzer, J. W. P., Gutzow, I. and Schmelzer Jr., J.: Curvature-Dependent Surface Tension  
10 and Nucleation Theory, J. Colloid Interf. Sci., 178, 657-665, 1996.
- 11 Schwier, A. N., Viglione, G. A., Li, Z. and McNeill, V. F.: Modeling the surface tension of  
12 complex, reactive organic-inorganic mixtures, Atmos. Chem. Phys. Discuss., 13, 549-580,  
13 2013.
- 14 Serry, F. M.: Improving the Accuracy of AFM Force Measurements: The Thermal Tune  
15 Solution to the Cantilever Spring Constant Problem, 2010.
- 16 Uddin, M. H., Tan, S. Y. and Dagastine, R. R.: Novel Characterization of Microdrops and  
17 Microbubbles in Emulsions and Foams Using Atomic Force Microscopy, Langmuir, 27,  
18 2536-2544, 2011.
- 19 Wex, H., Petters, M. D., Carrico, C. M., Hallbauer, E., Massling, A., McMeeking, G. R.,  
20 Poulain, L., Wu, Z., Kreidenweis, S. M. and Stratmann, F.: Towards closing the gap between  
21 hygroscopic growth and activation for secondary organic aerosol: Part 1- Evidence from  
22 measurements, Atmos. Chem. Phys., 9, 3987-3997, 2009.
- 23 Yazdanpanah, M. M., Hosseini, M., Pabba, S., Berry, S. M., Dobrokhотов, V. V., Safir, A.,  
24 Keynton, R. S. and Cohn, R. W.: Micro-Wilhelmy and Related Liquid Property  
25 Measurements Using Constant-Diameter Nanoneedle-Tipped Atomic Force Microscope  
26 Probes, Langmuir, 24, 13753-13764, 2008.

27

28



1 Table 1. Surface tension of bulk liquids used for standardization, measured by the Wilhelmy  
2 plate. Averages reported as “average +/- standard error.” Pure oleic acid has a surface  
3 tension of 32.79 dyn/cm at 20 degrees C (Chumpitaz et al., 1999), and pure  $\alpha$ -pinene has a  
4 surface tension of 26.0 dyn/cm at 25 degrees C (Daisey and Hopkey, 1993). Measured values  
5 on Wilhelmy plate are reasonably close to reported values, considering differences in purity  
6 and temperature.

7

<b>Component</b>	<b>Surface Tension (dyn/cm)</b>
Oleic Acid (90% purity)	29.47 29.53
<b>Average</b>	<b>29.50±0.03</b>
$\alpha$ -pinene (97% purity)	25.75 25.36
<b>Average</b>	<b>25.6±0.2</b>

8

9

10

11



1 Table 2. Measured and calculated values obtained during three experiments. In the first  
 2 experiment,  $\alpha$ -pinene was used as the standard, oleic acid was used as a check standard, and  
 3 the oxidized  $\alpha$ -pinene particles were generated in dry conditions. In the second experiment,  
 4 oleic acid was used as the standard, there was no check standard, and the oxidized  $\alpha$ -pinene  
 5 particles were generated in dry conditions. In the third experiment,  $\alpha$ -pinene was used as the  
 6 standard, there was no check standard, and the oxidized  $\alpha$ -pinene particles were generated in  
 7 wet conditions.

Experimental conditions	Standard		Check Standard		Sample Oxidized $\alpha$ -pinene particles	
	Measured Maximum Force (nN)	Calculated Wetted Tip Perimeter (nm)	Measured Maximum Force (nN)	Calculated Wetted Tip Perimeter (nm)	Measured Maximum Force (nN)	Calculated Surface Tension (dyn/cm)
-Particles generated at <10% RH	9.7	377.0	11.0	373.8	10.1	26.8
-Standard: $\alpha$ -pinene (97% purity)	9.6	373.8	10.9	370.7	10.2	27.0
-Check Standard: Oleic Acid (90% purity)	9.7	377.0	10.8	364.4	11.4	30.2
<b>Average</b>	<b>375.9±1.1</b>		<b>369.7±2.8</b>		<b>27.8±0.6</b>	
-Particles generated at <10% RH	11.7	395.8			10.8	27.2
-Standard: Oleic Acid (90% purity)	11.8	399.0			10.6	26.7
-Check Standard: None	11.7	395.8			10.6	26.8
<b>Average</b>	<b>369.9±1.0</b>				<b>26.9±0.2</b>	
-Particles generated at 67% RH	12.7	496.4			21.4	43.3
-Standard: $\alpha$ -pinene (97% purity)	12.5	490.1			21.2	42.9
-Check Standard: None	12.6	493.2			20.6	41.8
<b>Average</b>	<b>493.2±1.8</b>				<b>44.4±1.1</b>	

8

9

10



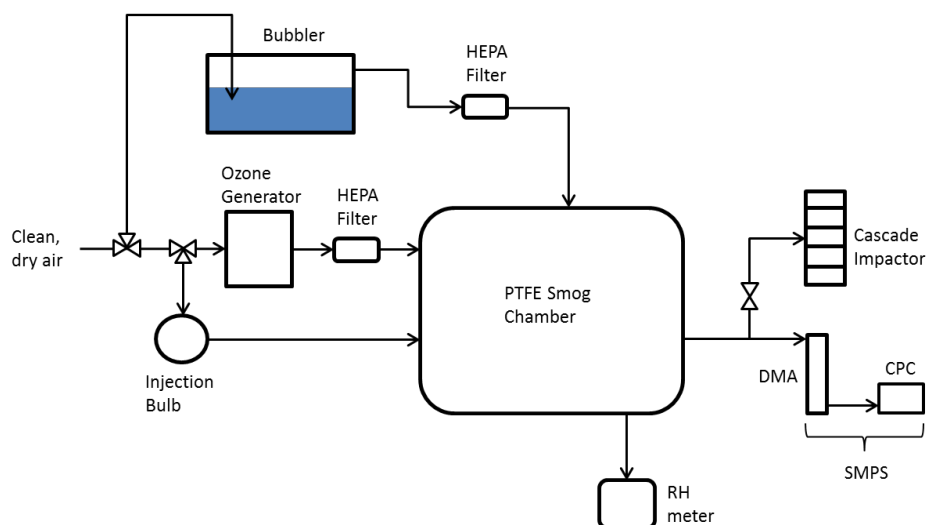
1

2 Table 3. Measured and approximated surface tensions of  $\alpha$ -pinene particles. Bulk  $\alpha$ -pinene and dry,  
3 oxidized  $\alpha$ -pinene particles have a similar surface tension. Wet  $\alpha$ -pinene particles have a higher  
4 surface tension.

5

RH at particle creation (%)	Surface tension (dyn/cm)	Description, Source
n/a	<b>25.6</b>	Pure $\alpha$ -pinene, bulk This experiment; Wilhelmy plate
<10	<b>27.5</b>	Oxidized $\alpha$ -pinene particles This experiment; AFM measurements
67	<b>44.4</b>	Oxidized $\alpha$ -pinene particles This experiment; AFM measurements
100 (Activation)	<b>61.7</b>	Oxidized $\alpha$ -pinene particles, assume depressed surface tension of pure water Engelhart et al., 2008
100 (Activation)	<b>72.5</b>	Oxidized $\alpha$ -pinene particles, assume surface tension of pure water Huff Hartz et al., 2005; Prenni et al., 2007

6

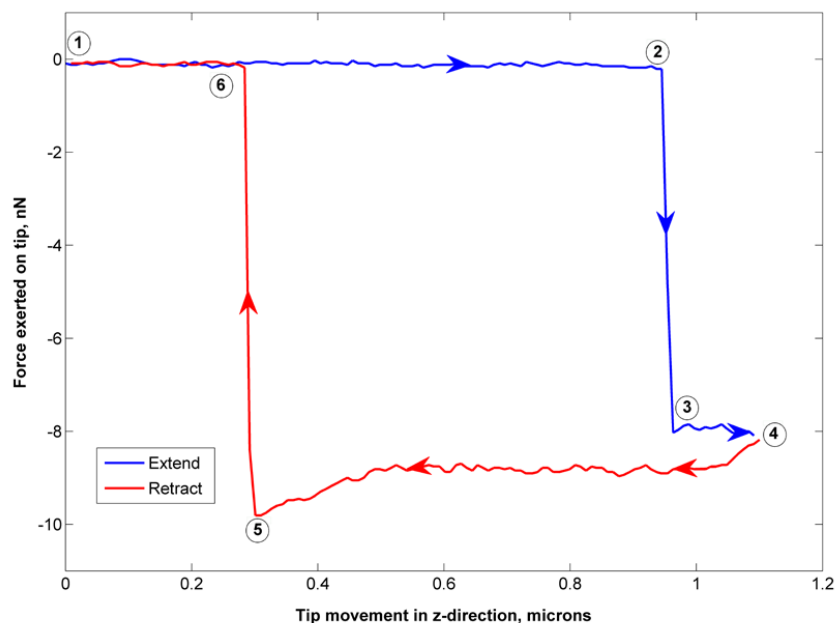


1

2 Figure 1. Experimental setup used to generate and collect oxidized  $\alpha$ -pinene particles. The  
3 smog chamber is initially flushed with dry or wet air. Once the relative humidity in the  
4 chamber is established, particles are generated in the smog chamber by mixing  $\alpha$ -pinene and  
5 ozone. Resulting particles are either analyzed with the SMPS or sampled using the cascade  
6 impactor.

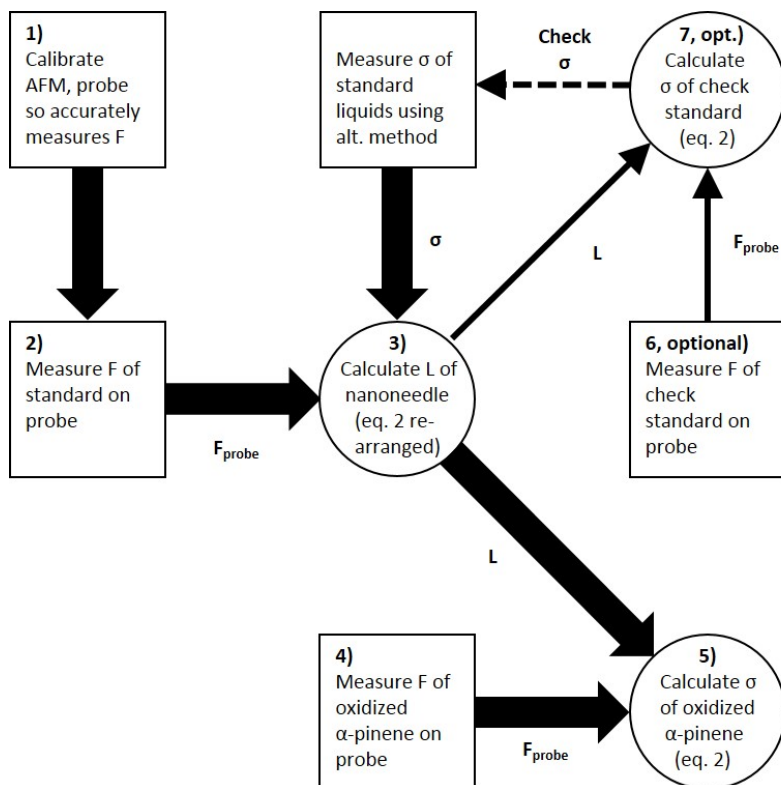
7





1

2 Figure 2. A typical force curve obtained using NaugaNeedle NN-HAR-FM60 probes and an  
3 atomic force microscope. The blue line indicates the probe approaching the sample, and the  
4 red line indicates the probe retracting from the sample. At point 1, the nanoneedle is  
5 approximately 1 micron from the surface of the liquid sample. At point 2, the nanoneedle is  
6 just above the surface of the liquid. At point 3, the nanoneedle has touched the liquid, which  
7 wicks up and exerts a downward force on the probe. At point 4, the nanoneedle begins to pull  
8 out of the liquid. At point 5, the liquid is just about to break from the end of the nanoneedle,  
9 and the contact angle of the liquid-needle interface approaches zero. At point 6, the  
10 nanoneedle has pulled out of the liquid sample. The probe retracts back to point 1.



1

2 Figure 3. Procedure used to determine the surface tension of oxidized  $\alpha$ -pinene particles using  
3 the AFM. The cantilever's spring constant was determined (step 1), which allowed the AFM  
4 to obtain force curves. Force curves of a liquid standard were obtained (step 2), and the  
5 nanoneedle's wetted perimeter was calculated with equation 2 given the standard's known  
6 surface tension (step 3). Force curves of the oxidized  $\alpha$ -pinene sample were obtained (step 4),  
7 and its surface tension was calculated with equation 2 given the nanoneedle's wetted  
8 perimeter (step 5). For initial tests, a check standard was used to verify the validity of the  
9 wetted perimeter and sample surface tension calculations (optional steps 6-7).